

Siamak G. Faal

Soft Robotics Laboratory,
Department of Mechanical Engineering,
Worcester Polytechnic Institute,
100 Institute Road,
Worcester, MA 01609
e-mail: sghorbanifaal@wpi.edu

Fuchen Chen

Soft Robotics Laboratory,
Department of Mechanical Engineering,
Worcester Polytechnic Institute,
100 Institute Road,
Worcester, MA 01609
e-mail: fchen@wpi.edu

Weijia Tao

Soft Robotics Laboratory,
Department of Mechanical Engineering,
Worcester Polytechnic Institute,
100 Institute Road,
Worcester, MA 01609
e-mail: wtao@wpi.edu

Mahdi Agheli

Soft Robotics Laboratory,
Department of Mechanical Engineering,
Worcester Polytechnic Institute,
100 Institute Road,
Worcester, MA 01609
e-mail: mmaghelih@wpi.edu

Shadi Tasdighikalat

Soft Robotics Laboratory,
Department of Mechanical Engineering,
Worcester Polytechnic Institute,
100 Institute Road,
Worcester, MA 01609
e-mail: stasdighikalat@wpi.edu

Cagdas D. Onal¹

Soft Robotics Laboratory,
Department of Mechanical Engineering,
Worcester Polytechnic Institute,
100 Institute Road,
Worcester, MA 01609
e-mail: cdonal@wpi.edu

Hierarchical Kinematic Design of Foldable Hexapedal Locomotion Platforms

Origami-inspired folding enables integrated design and manufacturing of intricate kinematic mechanisms and structures. Here, we present a hierarchical development process of foldable robotic platforms as combinations of fundamental building blocks to achieve arbitrary levels of complexity and functionality. Rooted in theoretical linkage kinematics, designs for static structures and functional units, respectively, offer rigidity and mobility for robotic systems. The proposed approach is demonstrated on the design, fabrication, and experimental verification of three distinct types of hexapedal locomotion platforms covering a broad range of features and use cases. [DOI: 10.1115/1.4030468]

1 Introduction

Mechatronic and robotic development demands new design and fabrication techniques for mechanical systems to address open challenges regarding the assembly process, speed, and cost of traditional approaches. Advances in electronics and reduced size of components provide a potential to combine the mechanical and electrical subsystems in a unified assembly process. While layer-by-layer 3D printing can fabricate highly complicated parts and assemblies, the manufacturing and assembly processes are time-consuming and costly, while circuit integration remains a significant challenge. As a potential solution, origami-inspired foldable structures are fabricated from thin sheets of raw material using

planar manufacturing and subsequent folding techniques [1–3]. The process includes cutting a crease pattern and folding the structure based on given blueprints. Cutting the crease patterns through the sheet of material, which is usually performed with laser cutters, is a rapid and inexpensive process. Also, the material sheets in flat form can be equipped with electrical components before assembly. This will significantly reduce the storage and shipping volume of the products. Application of origami-inspired foldable structures enables the construction of complicated assemblies that contain both mechanical and electrical components. As a consequence, robotic systems with fully integrated circuitry and motion transmission elements can be developed from scratch at scales and volumes not achievable by existing techniques.

With the advances in self folding structures [4–8], folding can happen through a human-independent process. Thus, fabrication methods that involve folding are a promising solution for fast and inexpensive on-demand productions. A significant problem

¹Corresponding author.

Manuscript received August 16, 2014; final manuscript received April 15, 2015; published online August 18, 2015. Assoc. Editor: Aaron M. Dollar.

associated with foldable techniques is the design of crease patterns. The crease patterns need to address the geometrical as well as mechanical requirements of the parts. This paper addresses the design process of simple and complex structures using a novel hierarchical approach. To assist the design process, a growing library of fundamental building blocks and corresponding crease patterns are introduced that can be combined to form increasingly complex units and structures. The approach discussed in this article is on semantic and functional design modulation and it is different from design synthesis based on computational search algorithms that are discussed in Refs. [9,10]. As an application of the introduced technique, three different hexapod platforms are considered to address the design of simple, as well as complex structures with multiple degrees of freedom (DOF).

To be able to perform real services, robots need to have a dexterous and agile locomotion system. Inspired by the locomotion systems of insects [11], hexapod platforms are a promising solution to take the robots out of laboratory environments. The static stability with enough dexterity to pass over relatively rough and uneven terrain make hexapod platforms a suitable solution for outdoor applications [12,13]. For use as multirobot agents, fabrication of each one of the platforms needs to be cost- and time-effective [14,15]. To address this issue, this paper discusses three different designs for foldable hexapedal locomotion platforms, namely: (1) a 2DOF platform that utilizes two 6-bar linkages on both sides for differential steering; (2) a 3DOF mechanism that uses three 6-bar linkages to allow the system to exhibit three degrees of mobility (DOM) [16]; and (3) an 18DOF platform that is composed of six, 3DOF serial linkages. The origami techniques that are utilized in the design process reduces the time and cost of fabrication. In comparison to relatively rigid structures, the compliance of the materials that are used for folding and the flexibility of folded joints allow the structures to possess an inherent suspension system to absorb collisions between feet and substrate surface.

The main contributions of this paper can be outlined as: (1) marrying kinematic synthesis with origami engineering to achieve robotic mechanisms of arbitrary complexity. The applicability of the introduced techniques has been evidenced through the design and fabrication of three different multilegged robots, demonstrating the broad range of possibilities; (2) design, fabrication, and experimental verification of a novel holonomic 3DOF foldable legged platform. Unlike mecatum wheels [17], the holonomic legged architecture can be utilized on relatively rough terrain; (3) design and fabrication of an 18DOF foldable platform for service applications. This paper focuses on a novel design and fabrication process appropriate to create origami-inspired foldable robots of arbitrary complexity. Unlike the origami-inspired robots presented in the literature, the introduced hierarchical design process and functional units, allow fabrication of folded platforms with the desired mechanical and functional complexity according to task specifications. The presented robot prototypes are working examples of the proposed hierarchical design process to fabricate platforms, utilizing open- and closed-loop kinematic chains.

The rest of the article is organized as follows. Section 2 introduces the fundamental building blocks of foldable structures and discusses a basic hierarchical foldable design concept. Sections 3–5 cover the conceptual operation, design process, fabrication, and experimental results of 2, 3, and 18DOF foldable hexapedal locomotion platforms, respectively. The paper is concluded with discussions and future work in Sec. 6.

2 Building Blocks of Foldable Bodies

This section discusses fundamental building blocks used to design and fabricate foldable robotic platforms. Building blocks are categorized into two classes of: basic structures and functional units. Basic structures include rigid members, flexural joints, and connectors. Functional units are specific assemblies of basic structures to offer a growing variety of desired functionality.

Depending on the specific kinematic combination of basic structures, functional units can replicate a complex rigid body or a mechanism with specific DOF. In a hierarchical manner, the combination of functional units form mechanisms with arbitrarily high complexity.

2.1 Basic Structures. Our approach to origami-inspired foldable design and fabrication relies heavily on a set of basic structures, which include triangular hollow beams, flexural revolute joints, key-and-slot fasteners, and insertion locks. Triangular beams and flexures have been used extensively in multiple fields, since they are elegant formations to support loads and construct revolute joints, respectively. Key-slot fasteners and insertion locks are essential to maintain physical integrity of the as-folded 3D structures. This class of basic structures is sufficient to form relatively simple assemblies, which may yield a single, unified crease pattern. The 2DOF hexapedal platform detailed later is an example of only utilizing basic structures in the design to achieve complicated kinematic linkage systems through folding. We consider these basic structures as the fundamental building blocks necessary to create static structures and kinematic mechanisms useful for robotic systems.

2.1.1 Rigid Triangular Beams. Triangular beams are introduced to overcome the inherent flexibility of the thin raw materials (typically 0.127–0.254 mm thick plastic films [1]). Figure 1(a) illustrates an equilateral triangular beam, its corresponding crease pattern, and dimensional parameters. As discussed in Sec. 2.1.2, basic folds create flexures to replicate the behavior of revolute joints. Thus, any hollow beam structure that has more than three sides will have positive DOF, which defeats the purpose of introducing rigidity. The bending stiffness of a hollow triangular beam with thin walls is defined as

$$k_b = \frac{3Ew^3t}{4L^3} \quad (1)$$

where E is the Young's modulus (elastic modulus) of the material used, and L , w , and t are the length, width, and thickness of each face of the triangular beam, respectively, assuming that the embedded key-and-slot fasteners hold the shape rigidly. Thus, folding a triangular beam increases the bending stiffness of a strip of material by at least 3 orders of magnitude, which enables the treatment of these beams as kinematic links.

2.1.2 Flexural Revolute Joints. Flexural joints are achieved by taking advantage of the inherent flexibility of thin films. Figures 1(b) and 1(c) illustrate two basic formations that approximate the behavior of a revolute joint based on flexures [18]. As highlighted in Fig. 1(b), the dashed patterns are perforations, used to reduce the stiffness of the material at the fold line to a fraction of the bending stiffness of a solid strip to approximate a well-defined revolute joint [2]. While many planar fabrication processes are applicable, our work uses CO₂ lasers for rapid and low-cost manufacturing.

2.1.3 Key-Slot Fasteners. The main function of the key-slot fasteners is to keep the folds from unfolding, but they can be also used to connect or form a joint between two sections of the design. Different applications of the keys and slots are depicted in Fig. 1. Through experimentation, we concluded that using a trapezoidal shape for the keys significantly eases the folding process. During the insertion of a key into a slot, the two triangular sides of the key fold back to form a smaller rectangular key. After insertion, the folds open again and fixes the key in the slot. The flexibility of the connection point depends on the length of the key and the tolerances used during the planar design and fabrication process.

2.1.4 Insertion Locks. Similar to key-slot fasteners, insertion locks are useful to secure two separate units to each other.

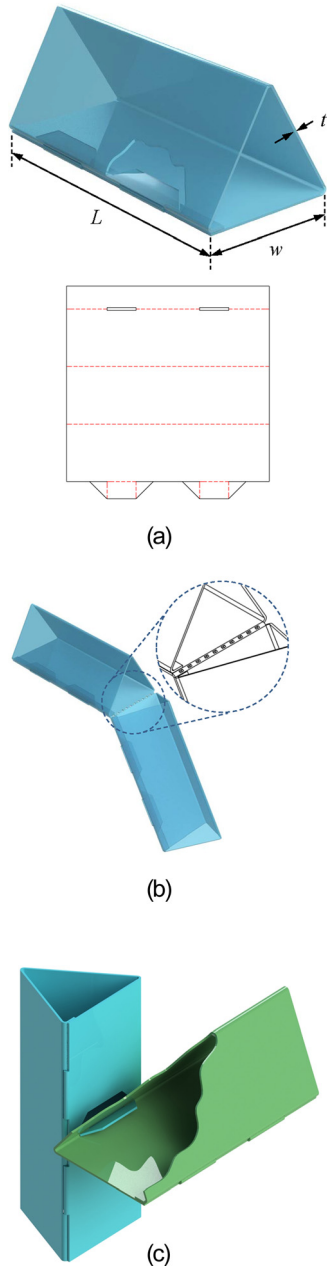


Fig. 1 The basic structures used in the design of the foldable platforms. (a) The triangular beam and the corresponding crease pattern. The cut in the beam shows how the keys and slots are used to keep the beam from unfolding. (b) Folded joint that resembles the effect of a revolute joint. The hollow patterns are added to reduce the stiffness of the material at the joint. (c) Another method of forming a revolute joint using only a key and a slot. The cut in the beam shows the slot and the key that is locked inside it.

Although locks are composed of starlike keys and slots, they do not require any preassembly folding as the locking process happens automatically by the insertion of the first unit with slots inside the starlike patterned keys of the second unit. The assembly process of a lock is depicted in Fig. 2. As shown in this figure, the starlike keys penetrate into the allocated slots and fastens the units to each other.

2.2 Functional Units. Forming functional units from basic structures reduces the complexity of the design process. The functional units do not necessarily need to be fabricated individually.

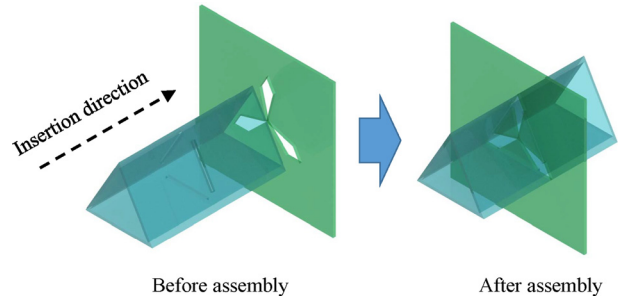


Fig. 2 The typical structure and assembly process of an insertion lock

As discussed in the flowchart of Fig. 3, it might be possible to combine the crease patterns of functional units into a unified pattern. On the other hand, fabricating functional units individually can significantly reduce the constraints in the design and assembly process. Typically, the design of a unified single crease pattern from scratch requires significant expertise, while composition of functional units is routinely performed by novice researchers in our group. Moreover, the modular nature of functional units lends itself to rapid modifications without redesigning the entire system. Depending on the structures used, functional units can have zero, as well as, multiple DOF. As an example, connecting three triangular beams to each other yields trusslike formations, which is a static unit that can tolerate large loads. On the other hand, connecting multiple beams and joints form linkage mechanisms, which can serve a specific purpose. Note that, with this approach, it is possible to create both serial and parallel kinematic mechanisms as functional units. While linkage mechanisms of any configuration can be achieved with our approach, we pay special

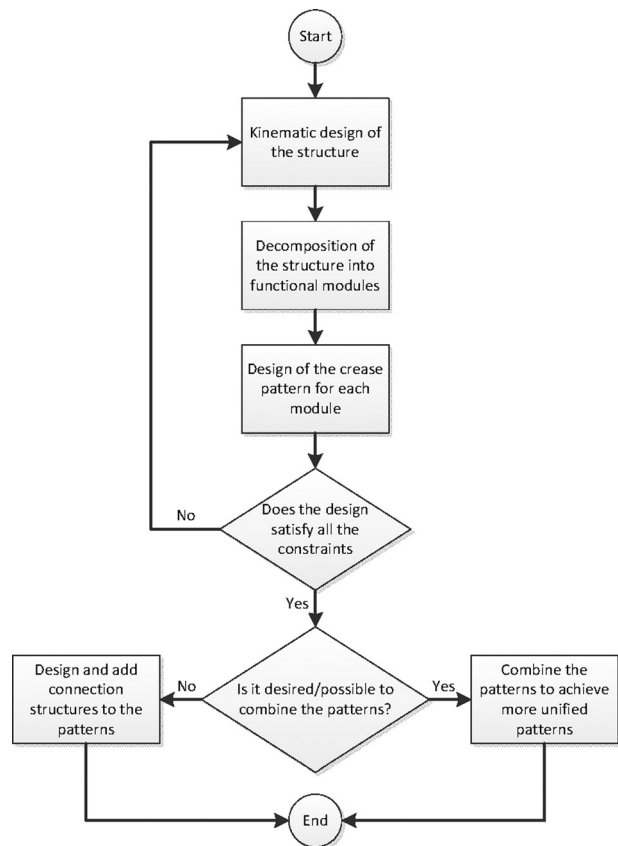


Fig. 3 Design process flow chart that represents the major foldable structure design steps

attention to the 6-bar, as an extremely versatile motion output unit, which can be tuned to produce a wide range of functions [19].

As described later, the 3DOF platform utilizes an active functional unit that is a 6-bar linkage. The connection of three of these units, forms the platform, while the static base is formed by a truss unit. Similarly, the 18DOF platform is an example of using different static units. Each static unit is a beam that is designed to hold a servomotor on one side and to connect to another servomotor horn on the other side. Connecting the three separate units forms each leg of the robot. The main body of the platform is formed by the connection of six static units. Thus, combination of functional units is a promising approach to design and manufacture integrated robotic platforms, as described on three foldable hexapod mobile robots with case studies presented in Secs. 3–5.

2.3 Design Process. Based on the complexity of the overall structure, it may not be feasible to construct it from a unified crease pattern [20]. On the same note, it may be desirable to fabricate the structure from groups of subunits. This justification can be based on the space and complexity requirements of the storage and fabrication process.

Figure 3 describes our basic design process for origami-based foldable mechanical systems. As depicted in this figure, the design process starts with structure and kinematic synthesis of the system. In this phase, the designer can omit the constraints associated with folding techniques in order to finalize the initial concept. The process follows by decomposing the structure into functional subsections such as: independently actuated mechanisms, support structures, motor housings, etc. The next step is designing (or reusing existing) crease patterns for each one of the subsections. As discussed in Sec. 2.2, the crease pattern for each substructure is a functional unit and can be constructed from basic structures and combinations of other functional units.

At this stage, the designer can judge on the feasibility of the design based on constraints related to folding techniques. If it is not possible to construct a functional unit using folding techniques, either the overall design should be reconsidered, or that specific unit needs to be fabricated with an alternative process and assembled as discrete components. After designing all functional units, the designer can explore the possibility of combining the separate crease patterns into a unified pattern. On the other hand, if it is desirable to fabricate the assembly from discrete crease patterns, the next step will be designing the corresponding connections and joints between the functional units using key-slot fasteners and insertion locks.

2.4 Fabrication Material. Different materials such as fiber glass [4], carbon fiber [21], and posterboard [3] have been utilized in design and fabrication of foldable structures. Although utilizing a material with a relatively high stiffness improves the rigidity of the structure, it will be a poor choice for the joints. A common approach to provide the flexibility required at the joints is to use a sandwich of two materials, with relatively high and low flexibilities [3,21]. While the design and fabrication process can be generalized to utilize many different types of raw material, in systems discussed in this article, polyethylene terephthalate (PET) sheets with a thickness of 0.254 mm is considered as the main fabrication substrate. PET is relatively inexpensive, has low density, it is an electrical insulator and easy to cut with readily available technologies such as laser-cutter machines.

3 2DOF Hexapedal Locomotion Platform

While having more DOF may help mobile platforms to have higher dexterity, more actuators will dramatically increase the cost and complexity of the system. This makes the platform with higher number of active DOFs infeasible solutions, especially for multirobot applications. If the objective of the platform is to walk, turn, and maneuver over a relatively rough terrain, a legged robot

with two active DOFs will be sufficient, whereby the platform can move and rotate by controlling the speed of noncoinciding points of the body. The 2DOF platform in the present implementation is designed based on the same principle. Two 6-bar linkages, located on both sides of the platform, are responsible for legged locomotion. The role of 6-bar linkages is to control the speed of the robot, while providing it with static stability. The static stability of the system is achieved by guaranteeing that three feet contact the substrate surface throughout the gait cycle. A fully assembled 2DOF hexapod prototype and its control electronics is illustrated in Fig. 4.

3.1 Design. Six-bar linkages are realized by composing a 4-bar crank-rocker with a parallelogram linkage [19]. Figure 5 illustrates the complete 6-bar linkage annotated with all geometric parameters. The values assigned to these parameters are dominated by two factors: (1) the feasibility of the design to be fabricated by folding techniques; and (2) To guarantee the correct gait pattern. An optimization problem is formulated to find the optimal values for the design variables that will produce the maximum forward motion of the platform. This is achieved by minimizing the vibrations introduced to the motion due to the mismatch of the feet velocities. A perfect gait sequence is achieved when all the velocities of the active feet are in the same direction and parallel to the body of the platform. The active feet is defined as the link tips that are in contact with the ground. However, imposing this condition as a constraint to the optimization problem results in an

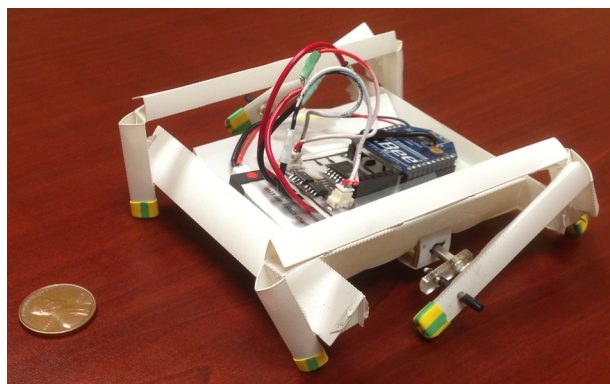


Fig. 4 Fully assembled 2DOF hexapod platform with on-board control electronics

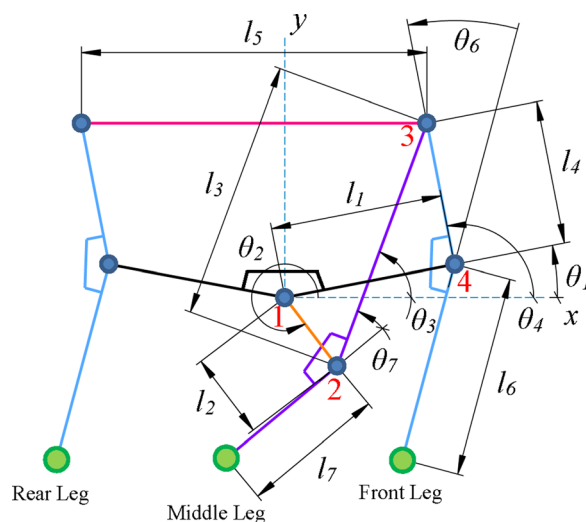


Fig. 5 All the parameters associated with the kinematics of the 6-bar linkage

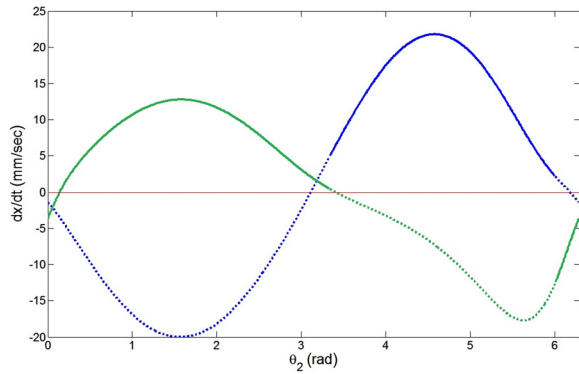


Fig. 6 The front (positive peak on the right) and middle (positive peak on the left) feet velocities along the x -axis. The solid lines represent the state of a feet as being active. Blue and green lines indicate the velocities of the front and middle foot, respectively.

empty feasible space. This conclusion has been made by running three different numerical optimization algorithms, from 500 different random initial points. To avoid this problem, the objective of the optimization is defined to maximize the distance traveled along the body of the robot by the active feet. The detailed description of the kinematics and the optimization formulations is presented in Ref. [14]. Note that this optimization is part of the kinematic design of the robot and it is independent of the general design procedure for foldable robotic systems. Here, we highlight the most significant parts of the process.

Design variables:

l_1, l_3 , and l_4

Constant values:

$l_2 = 20$ mm, $l_6 = l_7 = 15$ mm, $\theta_6 = \theta_7 = 0$ rad,
 $l_{\min} = 5$ mm: minimum feasible length of the links,
 $l_{\max} = 70$ mm: maximum feasible length of the links,

Dependent variables:

$l_5 = 2l_1$

Constraints:

g_1 to g_3 : $l_{\min} \leq l_i \leq l_{\max}, \forall i \in \{1, 3, 4\}$
 g_4 to g_6 : $l_2 - l_i + \varepsilon \leq 0, \forall i \in \{1, 3, 4\}$
 g_7 : $l_2 + S - \sum_i l_i + \varepsilon \leq 0$ for $S = \max\{l_1, l_3, l_4\}$ and $i \in \{1, 3, 4\} - \{i_S\}$
 g_8 : $\pi/6 \leq \theta_4 \leq 5\pi/6$

Objective function:

$$\text{Cost} = - \int v_{\text{ma}} \cdot e_x dt - \int v_{\text{fa}} \cdot e_x dt$$

where $v_{\text{ma}} \cdot e_x$ and $v_{\text{fa}} \cdot e_x$ are the velocities of the middle and front active feet of the platform along the x -axis, as depicted in

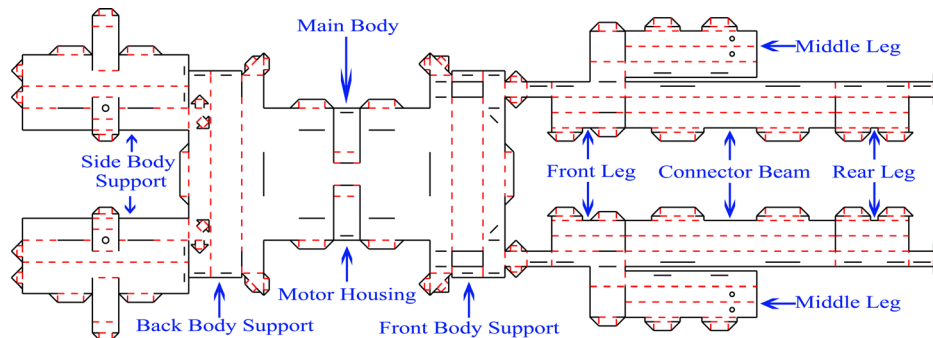


Fig. 7 The crease pattern of the 2DOF foldable hexapod robot. Solid and dotted lines indicate cut and fold lines, respectively.

Fig. 5. The constant values and constraints g_1, g_2, g_3 , and g_8 are defined based on the size requirements of the prototype. Constraints g_4 to g_6 are forcing l_2 to remain as the crank of the mechanism. The Grashof condition [19] is imposed by g_7 . The constraint g_8 is defined to keep the transmission angle in an acceptable range. To perform the optimization, two different optimization algorithms available in MATLAB software are used: the gradient based optimization and genetic algorithm. Due to the nonlinear nature of the problem, the numerical algorithms can not satisfy global optimality [22]. Thus, the optimization code is evaluated from different initial values to attain a set of solutions. After comparing the solutions, the one that has the minimum cost value is chosen as the final result.

Figure 6 illustrates the velocities of the front and middle feet, along the x -axis as functions of the crank angle, θ_2 for the final mechanism. Solid lines are used to indicate the state of the foot as being active. The blue and green colors are used to indicate the velocities of the front and rear feet, respectively. Since there are no constraints on the direction of the velocities during contact, there is an interval where the active foot has a negative velocity. Although this interval will cause jittering on the movement of the platform, the total integral of the velocities of the active feet for the optimal solution is considerably larger than zero. This means the platform will have a net displacement in the forward direction at each full rotation of the crank.

The crease pattern of the 2DOF hexapod is depicted in Fig. 7. Since this platform is designed by only utilizing simple structures, the final formation has a unified crease pattern. In this figure, solid black lines illustrate the cut lines, while the fold lines are illustrated by dotted red lines. Four triangular beams at each side of the base are used to provide it with the required rigidity. The two 6 bar mechanisms also utilize triangular folded beams as rigid links to offer the necessary strength under load.

3.2 Fabrication and Experimental Results. The fabrication process starts with laser machining the crease pattern on a sheet of PET with 0.254 mm thickness. Laser cutting the full pattern takes approximately 6 min. After cutting, the process continues by folding the crease pattern and assembling the external components such as DC-motors and control electronics. The overall manufacturing process takes less than 30 min. Nylon bands are used to cover the feet to increase traction.

A series of tests are conducted to validate the performance of the platform. The platform achieved a maximum forward velocity of 5 body lengths per second (approximately 0.5 m/s). It is observed that the forward velocity varies between this maximum speed and approximately half of the maximum speed due to a lack of synchronization between the left and right mechanisms. This lack of synchronization causes the gait sequence to periodically deviate from the tripod gait algorithm. This issue can be resolved by a suitable feedback control algorithm that synchronizes the speed of the two actuators. Figure 8 shows snapshots of the robot

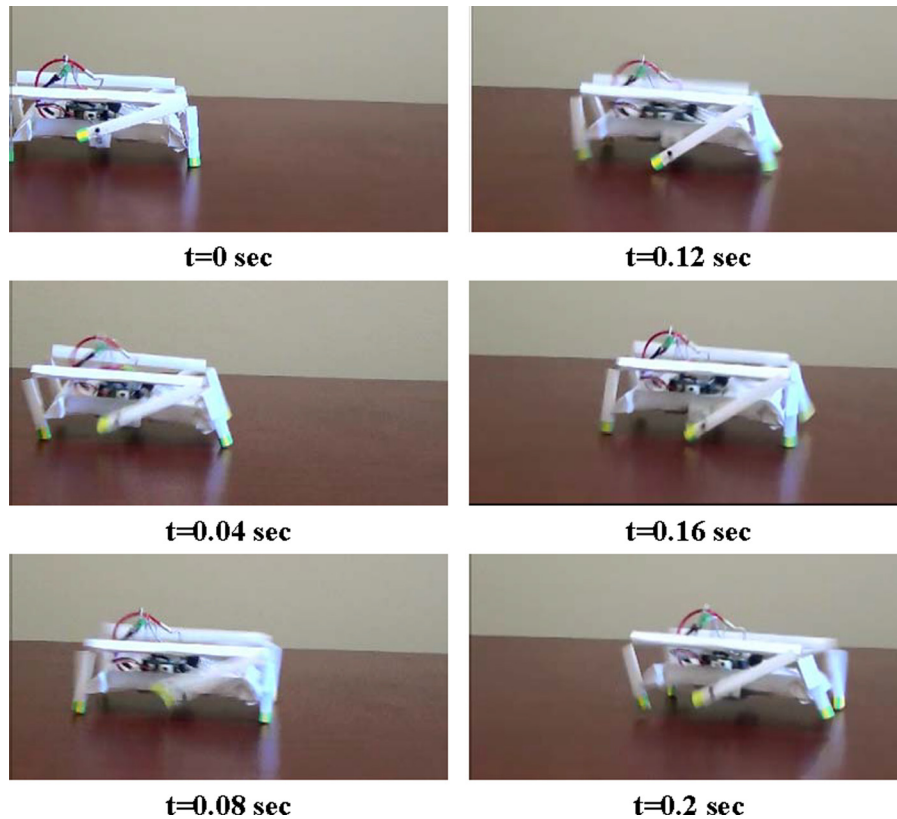


Fig. 8 Snapshots of the foldable hexapod robot prototype during a linear forward locomotion experiment

during a forward locomotion experiment going through a linear displacement of one body length. Since the platform has 2DOM, it can turn with zero radius of curvature. The maximum angular velocity of the robot was measured at approximately 2π radians per second. Figure 9 shows snapshots of the robot during an in-place turning experiment over an angular displacement of approximately 360 deg.

4 3DOF Hexapedal Locomotion Platform

The 3DOF platform is a novel design inspired by holonomic drive locomotion systems, but using coordinated motions of multiple legs instead of wheels. As a result, it can be suitable for applications that require 3DOM on a relatively rough surface. The platform is composed of three 6-bar linkages at each side of an equilateral triangle. Each mechanism is driven by a rotary actuator. Similar to holonomic drive systems, various linear and rotational motions are achieved by controlling the speed of each actuator. Figure 10 illustrates the fully fabricated platform with its control electronics.

4.1 Design. The design of the 6-bar linkages that are utilized in this platform are based on the Hoeken linkage [19]. The Hoeken linkage is a four-bar mechanism that is designed to convert rotational motion to an approximated straight-line motion with approximately constant velocity. The coupler curve of the linkage resembles the motion of a foot through a gait cycle. By taking advantage of this property, it is possible to produce gait patterns of the 3DOF platform. Note that, the link length ratios of the Hoeken linkage are modified to satisfy a relatively uniform speed profile with an elliptical coupler curve. To make the platform statically stable, each one of the 4-bar linkages is coupled with its cognate, that is 180 deg out of phase, to form a compact 6-bar linkage. Figure 11 illustrates the mechanism utilized in the 3DOF platform. The 180 deg phase difference allows one foot to

touch the ground as the other one is taking off. This effect is depicted in Fig. 11 using color-mapped coupler curves; where the colors depict the passage of time, from blue to red, also marked with arrows.

The design of the platform utilizes three units that are connected to each other to form an equilateral triangle. Each unit is composed of five different sections: a rigid triangular beam and four sections that shape the 6-bar mechanism. The three triangular beams of the three units form the central equilateral triangle base (kinematic truss structure) of the platform. Figure 12 illustrates crease patterns of different sections of one of the units.

4.2 Fabrication and Experimental Results. Similar to the 2DOF platform, the fabrication process initiates by laser cutting the polyester sheet. Laser cutting the full pattern takes approximately 10 min. The fabrication process continues by folding the crease pattern and assembling the external components. The overall fabrication process takes less than 40 min. To increase the traction between feet and the substrate surface, nylon bands are used to cover the feet.

The performance of the platform is tested through experimenting its holonomic locomotion system. Figure 13 displays the platform going through a triangular path. Note that, during this motion, the platform keeps its orientation approximately constant with less than ± 20 deg fluctuation for more than 90% through its motion, as depicted in Fig. 13. This motion is achieved by sequentially activating two of the three 6-bar linkages with the same velocity. It is observed that, during linear translation, the state of the inactive linkage may cause disturbances to the motion. This is due to the change of the contact point between the substrate surface and the inactive feet being dragged, which acts as a frictional steering force and leads to a slight rotation of the body, which can be corrected by feedback control. The relatively large orientation change observed in the last snapshot of Fig. 13 is suspected to be

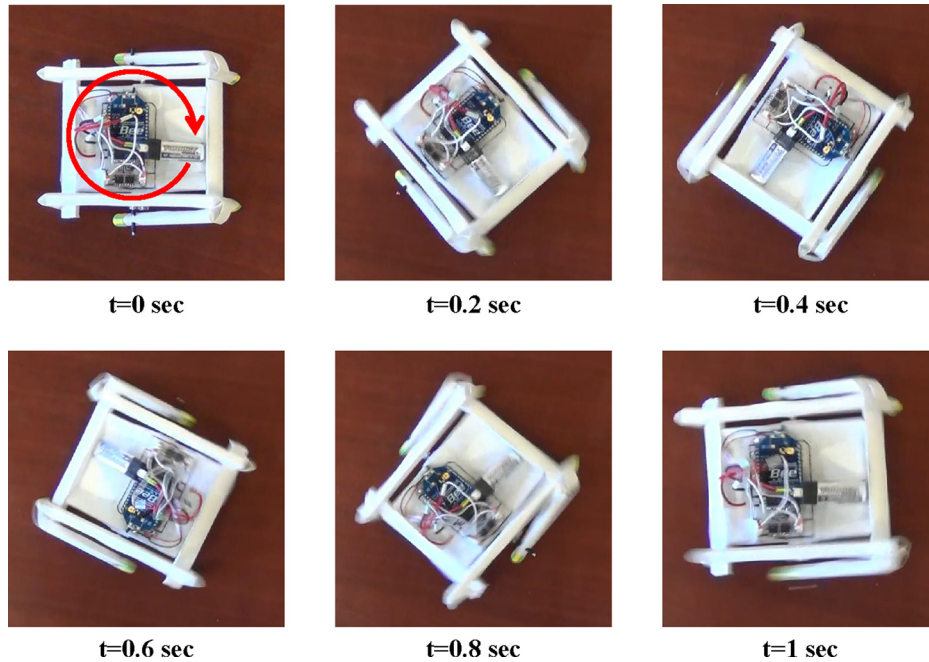


Fig. 9 Snapshots of the foldable hexapod robot prototype during an in-place turning experiment

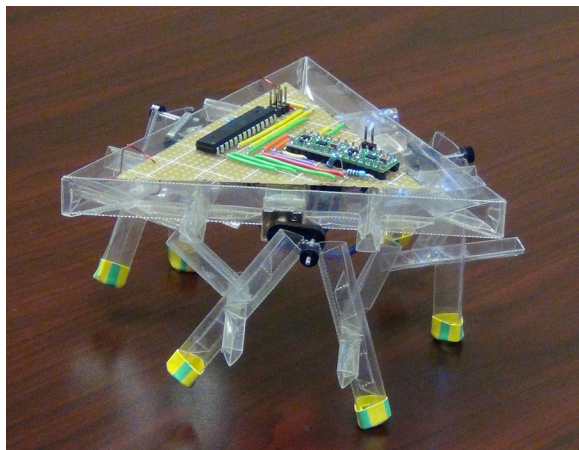


Fig. 10 Fully fabricated 3DOF hexapod platform with on-board control electronics

due to an external disturbance caused by irregularities on the substrate surface.

Similarly, the platform is capable of purely rotational motions by turning all three actuators in the same direction. Rotational performance was experimentally tested and the maximum angular velocity output was measured to be approximately 18 revolutions per minute. Figure 14 illustrates the 3DOF platform as it is rotating about an axis close to its geometrical center.

4.2.1 3DOF Mechanism Under Different Loading Conditions. The performance of the 3DOF robot mechanism for different loading conditions is tested experimentally. The experimental setup is composed of the folded 3DOF platform and a motion capturing system to record the motion of the tested foot. To conduct the experiment, the body of the robot is secured to a rigid surface with the legs pointing upward. Different weights of 20 g, 40 g, and 60 g are mounted on one of the feet sequentially to replicate the effect of the forces exerted to one of the legs during robot locomotion. Since the total mass of the robot is 59.2 g, and the total weight of the robot is supported by at least three legs, the weight

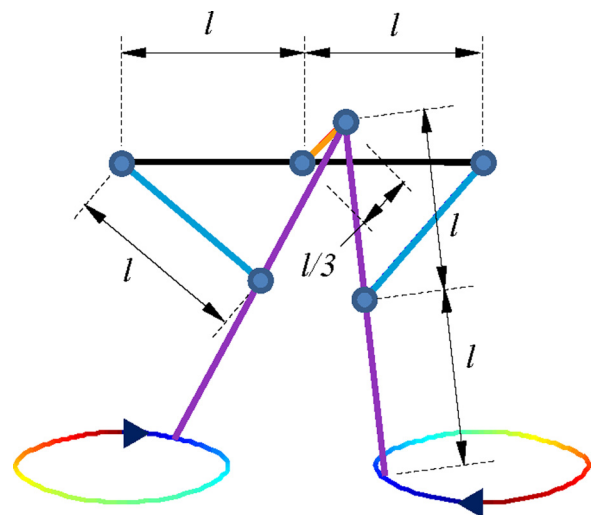


Fig. 11 The 6-bar mechanism that is used as the feet of the 3DOF platform. The shading of the coupler curves represent the passage of time. The arrows indicate motion direction.

values approximately represent total payloads of 1, 2, and 3 body weights. Figure 15 illustrates the results of this experiment. As observed in the figure, the mechanism reproduces the simulated coupler curve under no-load condition. As the amount of payload increases, the coupler curves shift toward positive x -axis (away from the other foot) and negative y -axis (gravity direction), i.e., payloads act to move the two feet apart from each other, as expected. The shifting effects are due to the moments and torsions exerted on the triangular beam of the base of the robot and indicate an inherent compliance that may act as a passive suspension system, which is a subject of further analysis in future work.

5 18DOF Hexapedal Locomotion Platform

The 18DOF hexapod platforms are interesting due to their high number of active DOF. The main body of the 18DOF hexapod is

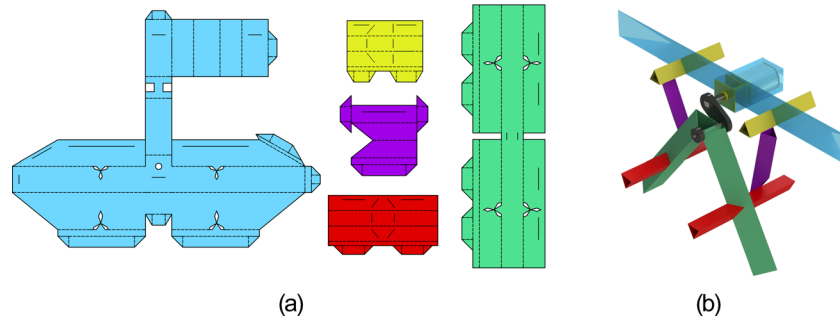


Fig. 12 (a) The crease patterns of the different sections of one of the units that form the 3DOF platform and (b) a 3D illustration of the folded patterns

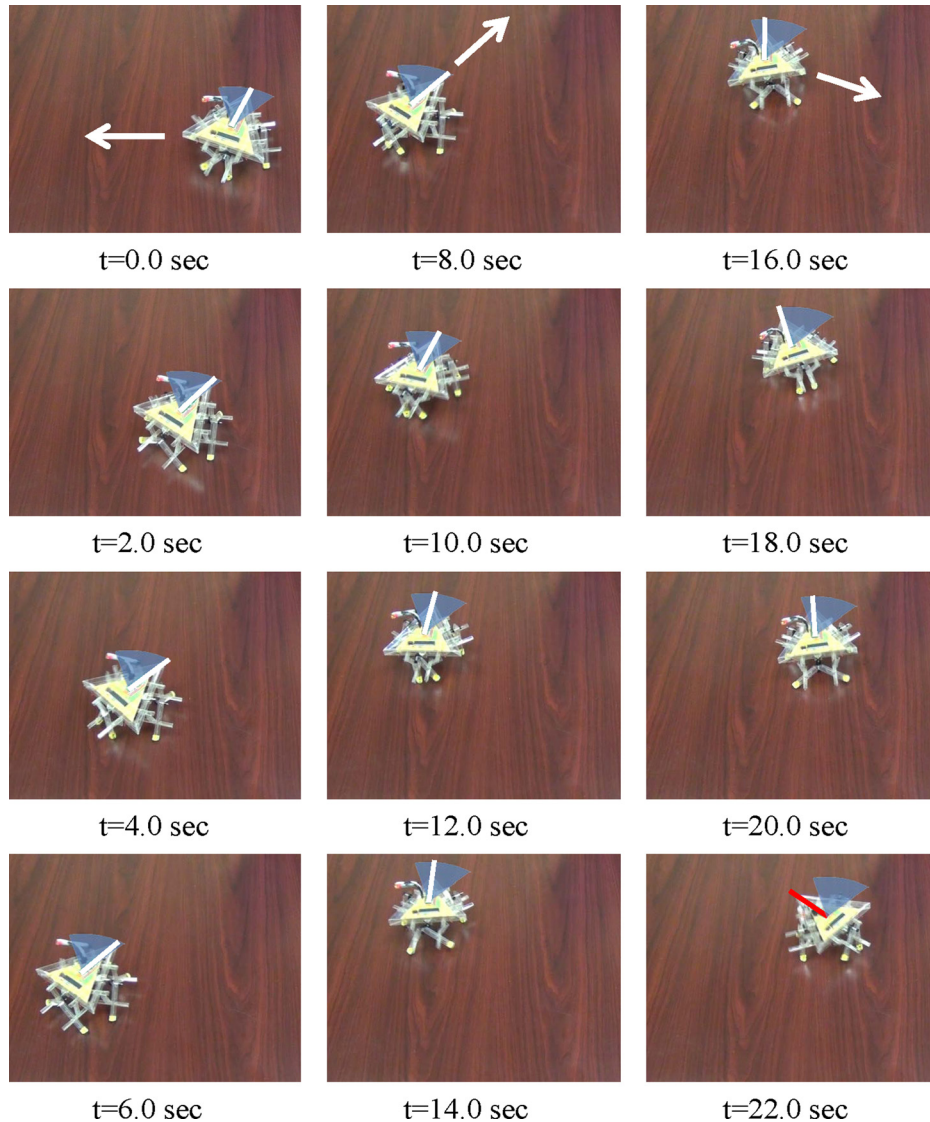


Fig. 13 Snapshots of the 3DOF hexapod platform going through a triangular path (depicted by arrows on the top row) by keeping its orientation (depicted by white lines) relatively consistent. Range of orientation changes due to imbalances in the body structure are depicted as an arc.

enclosed by six legs that each has 3DOF in a bisymmetric fashion. Thus, the main body has 6DOF in Cartesian space. Being able to have any orientation and position with respect to a fixed coordinate frame [23], makes 18DOF platforms a suitable solution for surveillance, remote sensing, manipulation, and many other

applications. The fully fabricated foldable 18DOF platform with the on-board control electronics is illustrated in Fig. 16.

5.1 Design. The DOF and different sections of one of the legs of the platform are illustrated in Fig. 17. As seen in this figure,

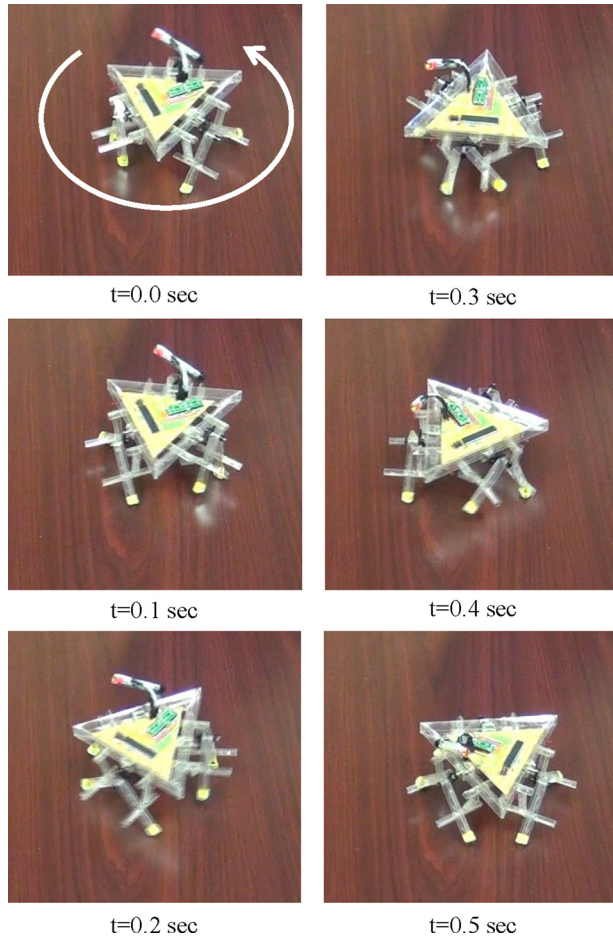


Fig. 14 Snapshots of the 3DOF platform rotating about an axis close to its geometrical center

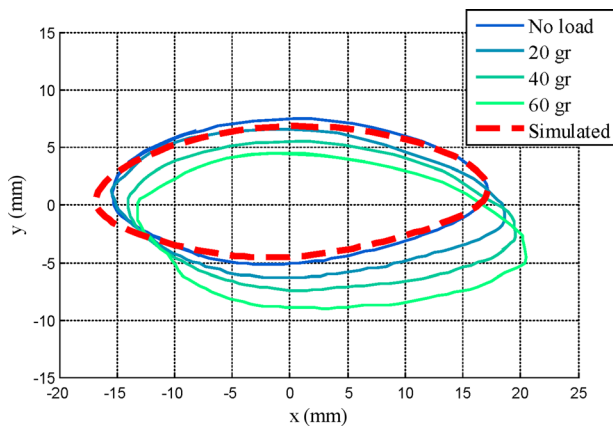


Fig. 15 The experiment result for different loading on the coupler point of the mechanism used in the design of the 3DOF hexapod robot

each leg is a serial linkage that is composed of three active DOF. Two of the joints have parallel axes of rotation, while the axis of the last joint is perpendicular to the other two. The structure of the platform is designed using four different static units. One of the units forms the central hexagon, while the other three are used as the coxa, femur, and tibia sections of each leg. Each leg section is connected to its neighbor section through the shaft of the actuators. Since the servomotors, used as the actuators of the platform, support each joint from one side, it is required to have an auxiliary shaft at each joint to support the free side. To address this issue, a



Fig. 16 The fully fabricated 18DOF platform with on-board control electronics

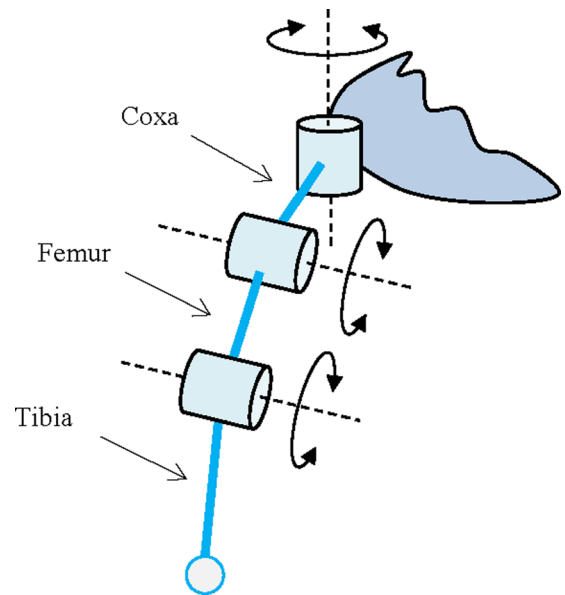


Fig. 17 The DOF of each leg of the 18DOF platform. The different sections of the leg are depicted in this figure.

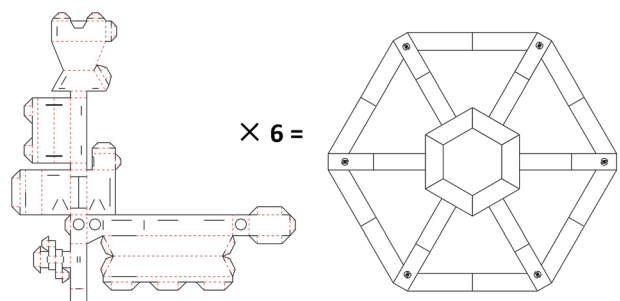


Fig. 18 The crease pattern for the units that create the hexagonal base of the 18DOF platform

pattern is added to each limb that provides it with a short and approximately round folded shaft. Figure 18 illustrates the crease pattern of the units that form the main body of the platform. The crease patterns of the leg sections are illustrated in Fig. 19. As mentioned before, solid black lines illustrate cuts and dotted red lines represent fold lines.

5.2 Fabrication and Experimental Results. Similar to the other platforms, fabrication process includes: laser cutting the

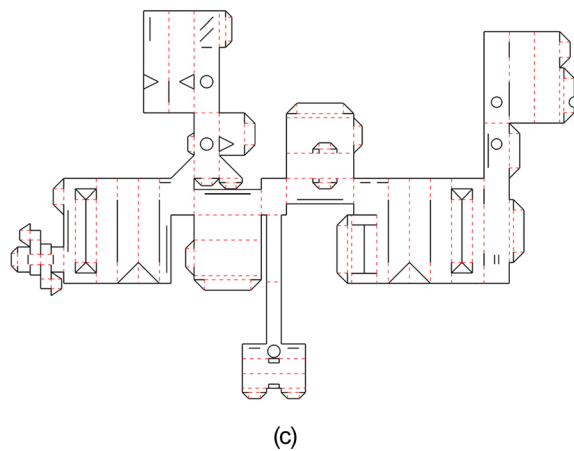
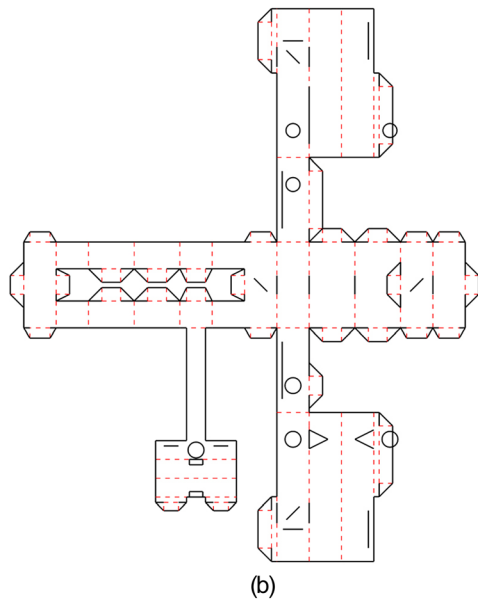
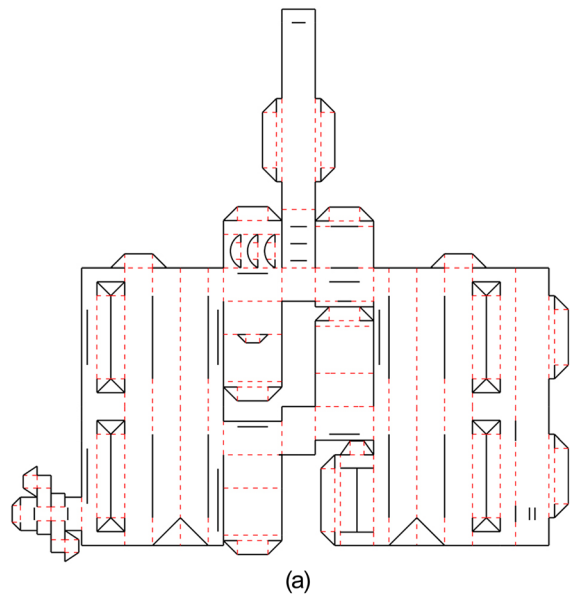


Fig. 19 The crease patterns for the coxa, femur, and tibia segments of each leg of the 18DOF

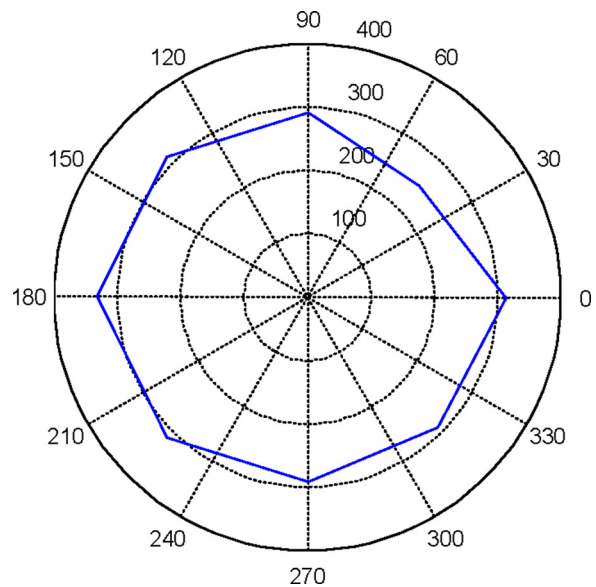


Fig. 20 Experimental walking performance of the 18DOF hexapod platform in eight directions with 45 deg increments using a wave gait. The total distance traveled after 25 steps, in millimeters, is depicted for each direction.

crease pattern on a polyester sheet, folding, and assembling the components. The cutting process takes approximately 10 min. It is possible to fold the whole structure within 2 hr. The assembly process takes longer, due to servomotor adjustments and wiring. The platform is tested with the hexapedal wave gait algorithm. The walking performance of the robot was tested in eight different directions relative to the main body of the robot with 45 deg increments, using the wave gait with a 0.75 duty factor. Figure 20 depicts the experimental travel distance of the robot after 25 steps in all eight directions. The asymmetry in traveled distances is related to small imperfections in the performance of off-the-shelf servomotors and an asymmetric mass distribution of the robot due to its off-centered battery pack.

6 Conclusions

A set of building blocks to design foldable structures is introduced and discussed. The techniques covered in the paper were applied to design and fabricate three different hexapod platforms as case studies. A 2DOF platform which is the least complex design to an 18DOF platform, which has the highest complexity. It is shown that by utilizing the proposed modular approach and the introduced building blocks, it is possible to design and fabricate structures with different levels of complexity. It is noticeable that these techniques are not limited to hexapod platforms and they can be applied to arbitrarily complex static or active systems with any number of DOF.

The three hexapod platforms introduced in this paper are meant to address different applications. The 2DOF platform is the most inexpensive and easy to fabricate platform, but it suffers from holonomic constraints on its mobility. Also, it is not possible to control the 3D orientation of the body of the platform with respect to the ground. The 3DOF platform demonstrates holonomic motion and it is suitable for applications, which require 3DOM. This effect can be utilized to move on a 2D surface without changing the orientation of the platform or to exert forces to an external object along any 2D direction. The 3DOF platform is also considerably simple and inexpensive. Thus, it can be a good candidate for multirobot or swarm applications. The 18DOF platform is the most complex structure among the three. Its complex crease pattern considerably increases the fabrication time. Also the 18 actuators, required to operate the joints, highly increases the final

cost and the power consumption of the system. On the other hand, the main body of the 18DOF platform has 6DOF in Cartesian space and can have any pose, position, and orientation, with respect to a fixed frame. Thus, this platform is suitable for surveillance and remote sensing applications, where it is needed to adjust a probe in a specific pose, for example.

The advantages of using foldable structures can be summarized as: low cost, fast and straightforward fabrication process, and structural compliance of the final product. Similar to any other fabrication method, foldable structures suffer from some limitations as well. The complexity of the crease patterns increases with the number of DOF of the system, making it difficult to design systems with high number of DOF to be fabricated from a unified crease pattern. The complexity of the crease pattern also makes it difficult to scale the design to different dimensions. Although foldable techniques can simplify the fabrication process of many systems, it may not be the most efficient solution for some applications. Most significantly, due to the nature of a fold, it is extremely difficult to have folded links that go through a full rotation. Thus, utilizing foldable techniques to design systems that have many parts going through full circular rotations is not trivial. In addition, the flexibility of the folded structure reduces the precision of the mechanisms. Although this flexibility highly helps with legged locomotion systems, it is an undesired feature for precision applications, such as manipulation. Ultimately, the proposed approach is a novel tool for the design and fabrication of future robotic systems to be incorporated with existing approaches, when advantageous for the requirements of the specific application.

References

- [1] Onal, C. D., Wood, R. J., and Rus, D., 2011, "Towards Printable Robotics: Origami-Inspired Planar Fabrication of Three-Dimensional Mechanisms," IEEE International Conference on Robotics and Automation (ICRA), Shanghai, May 9–13, pp. 4608–4613.
- [2] Onal, C. D., Wood, R. J., and Rus, D., 2012, "An Origami-Inspired Approach to Worm Robots," *IEEE Trans. Mechatronics*, **18**(2), pp. 430–438.
- [3] Hoover, A. M., and Fearing, R. S., 2008, "Fast Scale Prototyping for Folded Millirobots," IEEE International Conference on Robotics and Automation (ICRA 2008), Pasadena, CA, May 19–23, pp. 886–892.
- [4] Hawkes, E., An, B., Benbernou, N., Tanaka, H., Kim, S., Demaine, E., Rus, D., and Wood, R., 2010, "Programmable Matter by Folding," *Proc. Natl. Acad. Sci.*, **107**(28), pp. 12441–12445.
- [5] Felton, S. M., Tolley, M. T., Shin, B., Onal, C. D., Demaine, E. D., Rus, D., and Wood, R., 2013, "Self-Folding With Shape Memory Composites," *Soft Matter*, **9**(32), pp. 7688–7694.
- [6] Miyashita, S., Onal, C. D., and Rus, D., 2013, "Self-Pop-Up Cylindrical Structure by Global Heating," IEEE/RSJ International Conference on Intelligent Robots and Systems (IROS), Tokyo, Nov. 3–7, pp. 4065–4071.
- [7] Felton, S., Tolley, M., Demaine, E., Rus, D., and Wood, R., 2014, "A Method for Building Self-Folding Machines," *Science*, **345**(6197), pp. 644–646.
- [8] Silverberg, J. L., Evans, A. A., McLeod, L., Hayward, R. C., Hull, T., Santangelo, C. D., and Cohen, I., 2014, "Using Origami Design Principles to Fold Reconfigurable Mechanical Metamaterials," *Science*, **345**(6197), pp. 647–650.
- [9] Gao, W., Ramani, K., Cipra, R. J., and Siegmund, T., 2013, "Kinetogami: A Reconfigurable, Combinatorial, and Printable Sheet Folding," *ASME J. Mech. Des.*, **135**(11), p. 111009.
- [10] Mehta, A. M., and Rus, D., "An End-to-End System for Designing Mechanical Structures for Print-and-Fold Robots," IEEE International Conference on Robotics and Automation (ICRA 2014), Hong Kong, May 31–June 7, pp. 1460–1465.
- [11] Baisch, A. T., Sreetharan, P., and Wood, R. J., 2010, "Biologically-Inspired Locomotion of a 2g Hexapod Robot," IEEE/RSJ International Conference on Intelligent Robots and Systems (IROS), Taipei, Taiwan, Oct. 18–22, pp. 5360–5365.
- [12] Birkmeyer, P., Peterson, K., and Fearing, R. S., 2009, "Dash: A Dynamic 16g Hexapedal Robot," IEEE/RSJ International Conference on Intelligent Robots and Systems (IROS 2009), St. Louis, MO, Oct. 10–15, pp. 2683–2689.
- [13] Soltero, D. E., Julian, B. J., Onal, C. D., and Rus, D., 2013, "A Lightweight Modular 12-DOF Print-and-Fold Hexapod," IEEE/RSJ International Conference on Intelligent Robots and Systems (IROS), Tokyo, Nov. 3–7, pp. 1465–1471.
- [14] Agheli, M., Faal, S. G., Chen, F., Gong, H., and Onal, C. D., 2014, "Design and Fabrication of a Foldable Hexapod Robot Towards Experimental Swarm Applications," IEEE International Conference on Robotics and Automation (ICRA), Hong Kong, May 31–June 7, pp. 2971–2976.
- [15] Rubenstein, M., Ahler, C., and Nagpal, R., 2012, "Kilobot: A Low Cost Scalable Robot System for Collective Behaviors," IEEE International Conference on Robotics and Automation (ICRA), St. Paul, MN, May 14–18, pp. 3293–3298.
- [16] Siegwart, R., Nourbakhsh, I. R., and Scaramuzza, D., 2011, *Introduction to Autonomous Mobile Robots*, MIT Press, Cambridge, MA.
- [17] Diegel, O., Badve, A., Bright, G., Potgieter, J., and Thale, S., 2002, "Improved Mecanum Wheel Design for Omni-Directional Robots," Australasian Conference on Robotics and Automation, Auckland, Nov. 27–29, pp. 117–121.
- [18] Howell, L. L., 2001, *Compliant Mechanisms*, Wiley-Interscience, Hoboken, NJ.
- [19] Norton, R. L., 2004, *Design of Machinery: An Introduction to the Synthesis and Analysis of Mechanisms and Machines*, McGraw-Hill, New York.
- [20] Sung, C., Demaine, E. D., Demaine, M. L., and Rus, D., 2013, "Joining Unfoldings of 3D Surfaces," *ASME Paper No. DETC2013-12692*.
- [21] Wood, R., Avadhanula, S., Sahai, R., Steltz, E., and Fearing, R., 2008, "Microrobot Design Using Fiber Reinforced Composites," *ASME J. Mech. Des.*, **130**(5), p. 052304.
- [22] Arora, J., 2004, *Introduction to Optimum Design*, Academic Press, San Diego.
- [23] Agheli, M., and Nestinger, S. S., 2010, "Inverse Kinematics for Arbitrary Orientation of Hexapod Walking Robots With 3-DOF Leg Motion," 15th International Association of Science and Technology for Development (IASTED) Conference on Robotics and Applications (RA 2010), Cambridge, MA, Nov. 1–3, Paper No. 706-093.